JGR Planets

RESEARCH ARTICLE
10.1029/2024JE008403

Key Points:

- Hydrofracture in ice drives water-filled cracks downward due to the greater density of water
- Rapid hydrofracture is possible for realistic icy-moon stress configurations given a supply of meltwater and an initial fracture
- Hydrofracture allows surface-interior material transfer with implications for habitability and may be associated with chaos terrain genesis

Supporting Information:

Supporting Information may be found in the online version of this article.

Correspondence to:

R. Law,
robert.law@uib.no

Citation:

Law, R. (2025). Rapid hydrofracture of icy moon shells: Insights from glaciology. *Journal of Geophysical Research: Planets*, *130*, e2024JE008403. https://doi.org/10.1029/2024JE008403

Received 26 MAR 2024
Accepted 21 MAR 2025

Author Contributions:

Conceptualization: Robert Law
Formal analysis: Robert Law
Investigation: Robert Law
Methodology: Robert Law
Visualization: Robert Law
Writing – original draft: Robert Law
Writing – review & editing: Robert Law

Rapid Hydrofracture of Icy Moon Shells: Insights From Glaciology

Robert Law[1,2]

[1]University of Bergen, Bergen, Norway, [2]Bjerknes Centre for Climate Research, Bergen, Norway

Abstract Europa's surface exhibits many regions of complex topography termed "chaos terrains." One set of hypotheses for chaos terrain formation requires upward migration of liquid water from perched water bodies within the icy shell formed by convection and tidal heating. However, consideration of the behavior of terrestrial ice sheets suggests the upwards movement of water from englacial water bodies is uncommon. Instead, rapid downwards hydrofracture from supraglacial lakes—unbounded given a sufficient volume of water—can occur in relatively low tensile stress states given a sufficiently deep initial fracture due to the negative relative buoyancy of water. I suggest that downwards, not upwards, fracture may be more reasonable for perched water bodies but show that full hydrofracture is unlikely if the perched water body is located beneath a mechanically strong icy lid. However, full hydrofracture is possible in the event of lid break up over a perched water body and likely in the event of a meteor impact that generates sufficient meltwater and a tensile shock. This provides a possible mechanism for the transfer of biologically important nutrients to the subsurface ocean and the formation of chaos terrains.

Plain Language Summary Jupiter's moon Europa has a subsurface ocean surrounded by an icy shell that features numerous "chaos terrains" of jumbled topography. Most theories for the formation of chaos terrains focus on the upwards motion of water pooled within the icy shell, but this contrasts with the rapid downwards motion of water in ice sheets on Earth. This paper considers the rapid downwards motion of water on Europa and other icy moons through water-driven fracture (hydrofracture), finding that it is a possibility if a large water body is not covered by a strong lid. This has implications for delivery of biologically important material from the moon's surface to its ocean, and may help explain the formation of chaos terrains.

1. Introduction

The presence of liquid water in icy moons beyond the asteroid belt was hypothesized by Lewis (1971) and supported by surface images and magnetic field readings from the Voyager, Galileo, and Cassini satellite missions (Carr et al., 1998; Hendrix et al., 2019; Khurana et al., 1998; Lorenz et al., 2008; Porco et al., 2006). The presence of liquid water in these moons offers the tantalizing possibility of exobiology, which focussed research into whether the other basic requirements of chemical energy to drive metabolism and organic matter may also be met (e.g., Kargel et al., 2000; Sephton et al., 2018), with Jupiter's moon Europa receiving particular attention (e.g., Chyba & Phillips, 2001; NASA, 2017).

One pathway for the possibility of life on Europa requires the exchange of oxidants and organics produced on the moon's surface with the subsurface ocean (e.g., Carlson et al., 1999; Chyba, 2000; Chyba & Phillips, 2001; Delitsky & Lane, 1998), placing an emphasis on "chaos terrains" as possible locations for localized melting of Europa's icy shell (Carr et al., 1998; Thomson & Delaney, 2001) that may facilitate surface-ocean exchange. However, direct contact between a thin layer of brittle surface ice and an underlying ocean requires an unrealistic amount of thermal energy to locally melt Europa's icy shell (Collins et al., 2000; Goodman et al., 2004), the thickness of which is poorly constrained but may exceed 30 km (Billings & Kattenhorn, 2005; Fagents et al., 2022; Schenk, 2002; Sotin et al., 2002). Theories to explain chaos formation therefore frequently invoke the presence of a near surface water body emplaced through convective upwelling (e.g., Figueredo et al., 2002; Pappalardo & Barr, 2004; Schmidt et al., 2011; Sotin et al., 2002) upwards fracture of ice (Walker et al., 2021), or sills (Michaut & Manga, 2014) that then reach the surface through brittle fracture (e.g., Collins et al., 2000; Crawford & Stevenson, 1988; Luzzi et al., 2021; Manga & Wang, 2007; Singer et al., 2023). Perched (i.e., disconnected from the subsurface ocean) water bodies are required in these chaos terrain formation scenarios because the negative buoyancy of water with respect to ice means fractures propagating upwards from the

subsurface ocean would extend at most 90% of the way through the shell before reaching hydrostatic equilibrium (Crawford & Stevenson, 1988).

However, consideration of water bodies over ice sheets on Earth (supraglacial lakes) strongly suggests that the negative relative buoyancy of water presents a major problem to their stability. Antarctic ice shelves feature supraglacial lakes up to around 1 km in diameter, which are observed to drain rapidly through hydrofracture (Banwell et al., 2024; Dunmire et al., 2020; Robel & Banwell, 2019; Scambos et al., 2000; Warner et al., 2021). Such lakes also pepper the margins of the Greenland Ice Sheet, with 28%–45% readily observed to drain rapidly through hydrofracture (Chudley et al., 2019; Cooley & Christoffersen, 2017; Das et al., 2008; Doyle et al., 2013; Fitzpatrick et al., 2014; Williamson, Banwell, et al., 2018). Theoretical considerations, and in the case of Greenland resultant ice-sheet speed up due to basal lubrication, show that such fractures will reach the ice-ocean or ice-bed interface given a sufficient supply of water (Krawczynski et al., 2009; Van der Veen, 2007; Weertman, 1973). In these settings an initial fracture is required for drainage through hydrofracture to occur. This may come from tensile shock from nearby hydrofracture events (Christoffersen et al., 2018), a transient strain rate increase as a result of changes in the subglacial hydrological system (e.g., Poinar & Andrews, 2021), ice-shelf flexure (e.g., Banwell et al., 2013), or reactivation of an existing weakness (Chudley et al., 2019) though it is not clear that there is a single dominant statistically supported explanatory mechanism (Williamson, Willis, et al., 2018). Notably, supraglacial lakes on the Greenland Ice Sheet form in depressions in the ice surface which are generally dominated by compressive stresses (Chudley et al., 2019; Doyle et al., 2013; Stevens et al., 2015).

Slow density-driven downward transport of temperate ice (ice at the pressure-dependent melting point containing a small percentage of liquid water) through an icy moon shell has been considered as a mechanism that would limit the longevity of perched water bodies (Carnahan et al., 2022; Hesse et al., 2022; Kalousová et al., 2024; Karlstrom et al., 2014). Linear elastic fracture mechanics has furthermore been used to investigate downwards dry fracturing on Europa, and upwards fracturing from the ice-ocean interface (Craft et al., 2016; Lee et al., 2005; Poinelli et al., 2019; Rudolph & Manga, 2009). However, the possible implications of rapid downwards hydrofracture from perched water bodies have not thus far been explored. In this paper I cover two perched water body settings: one formed through convective and tidal heating (Figure 1a) and a second formed by a meteorite impact (Figure 1d). Each of these water bodies may then be separated from the ice surface by a mechanically strong ice layer (Figures 1b and 1e) or a weak melange of ice, water, and slush (Figures 1c and 1f), such as that commonly found in Greenlandic fjords (e.g., Todd & Christoffersen, 2014). Calculating the stresses governing hydrofracture in a simplified two-dimensional plane indicates that full-thickness hydrofracture is possible when a mechanically strong lid is not present, provided there is a sufficient supply of water. I suggest hydrofracture may be more likely in the event of a meteorite strike that also provides an initial fracture site. Such a mechanism may be associated with chaos terrain formation if violent drainage prompts surface collapse, providing a clear pathway for the transport of organics and oxidants into the subsurface ocean. I focus on Europa, but the results are applicable to any ice shell setting.

1.1. Materials and Methods

Van der Veen (1998) calculates water-filled terrestrial crevasse propagation under linear elastic fracture mechanics which treats a material as containing small defects which affect its load-bearing capacity. If high stresses concentrate near a defect the defect may propagate and ultimately fracture (Broek, 1982). In a purely elastic material, an unstable crack will propagate when the energy absorbed by a small expansion of the crack is exceeded by the energy released by a small increase in crack size (Griffits, 1921). This condition is met when the net stress intensity factor at the fracture tip, $K_{(\mathrm{net})}$ (Pa $\mathrm{m}^{1/2}$), exceeds the fracture toughness of the material. Ice is not a purely elastic material (instead it has a non-linear viscoelastic rheology and may be approximated as plastic at the fracture tip under very high stresses; Walker et al., 2021), but linear elastic fracture mechanics has proven effective in application to terrestrial ice sheets where temperatures are within 25 K of the pressure melting point throughout, and less than 10 K away from the pressure melting point in the zone of fracture initiation close to the surface (e.g., Chudley et al., 2019; Law et al., 2021; Van der Veen, 1998, covered further in the Discussion). Nonetheless, full inclusion of viscous effects will still improve model realism (Hageman et al., 2024). The outer shells of icy moons are likely much colder (down to 100 K at the surface, but at the pressure melting point at the shell-ocean boundary) and therefore stiffer than terrestrial ice (Ashkenazy, 2019; Goldsby & Kohlstedt, 2001; Hussmann et al., 2002) with a correspondingly increased Maxwell time (Lesage et al., 2022) making a focus on the elastic component only appropriate here, as in previous terrestrial and extraterrestrial studies (e.g., Lee

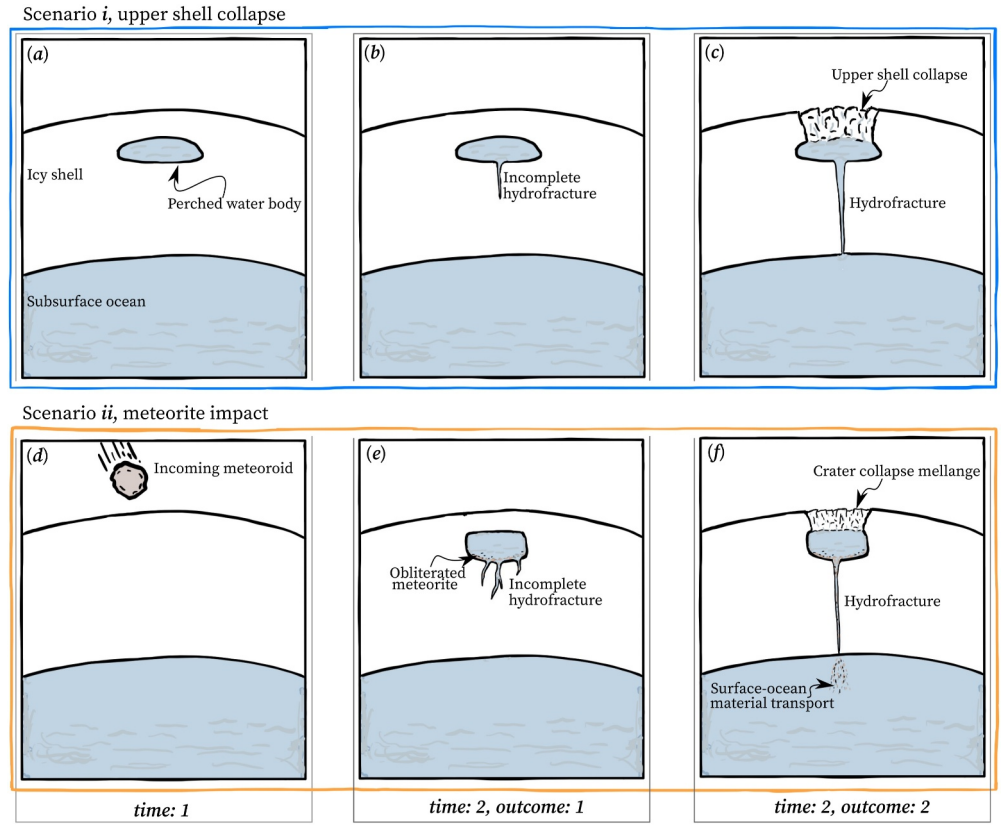

Figure 1. Schematic of icy-shell hydrofracture scenarios covered in the text. (a) A perched water body as hypothesized to form through thermal convection or a sill. (b) Incomplete hydrofracture in a perched water body with a rigid lid. (c) Collapse of the upper shell and full hydrofracture. (d) Incoming meteoroid. (e) Incomplete hydrofracture following meteorite impact. (f) Full hydrofracture of meteorite-generated meltwater when the surface is not sealed following meteorite impact.

et al., 2005; Poinelli et al., 2019). On Earth, melt-formed conduits are also ubiquitous in temperate ice alongside fractures (Fountain & Walder, 1998; Gulley et al., 2009) and surface water is still evacuated through several tens of meters of temperate ice at the bottom of an ice sheet (Chudley et al., 2019; Law et al., 2021).

The calculations below are separated into two parts. **First**, I use the essential equations from Van der Veen (1998) to calculate the stress states required for hydrofracture. **Second** I follow Weertman (1973) and Krawczynski et al. (2009) to calculate the volume of water required for hydrofracture. Considering first the stress states required for hydrofracture, I take a single water-filled fracture unaffected by surrounding fractures (Figure 2) and consider only Mode I fracturing where the fracture opens symmetrically as a result of stresses normal to the fracture plane. More closely spaced fractures will decrease the stress concentration at the fracture tip (Van der Veen, 2013), but consideration of supraglacial lake drainages suggests that where an abundant water source is present fractures quickly coalesce with depth (Chudley et al., 2021). In keeping with previous planetary and terrestrial studies (e.g., Craft et al., 2016; Lee et al., 2005; Rudolph & Manga, 2009; Van der Veen, 2007) and to conform with the assumptions of Broek (1982) I therefore exclude additional fractures to simplify calculations. Further, linear elastic fracture mechanics should only be considered strictly valid for cracks exceeding the area of plastic deformation at the fracture tip, which for this setting is around 2.5 m (Supporting Information S1; Walker et al., 2021).

The net stress intensity factor $K^{(\mathrm{net})}$ determines whether a fracture propagates if it exceeds the material fracture toughness, and is calculated as the sum of three processes: the far-field tensile or compressive stress (as $K^{(1)}$); the hydrostatic stress (as $K^{(2)}$); and water pressure (as $K^{(3)}$). $K^{(1)}$, $K^{(2)}$, and $K^{(3)}$ can be superimposed without complication unlike if Mode II and Mode III openings were also considered (Van der Veen, 1998), giving

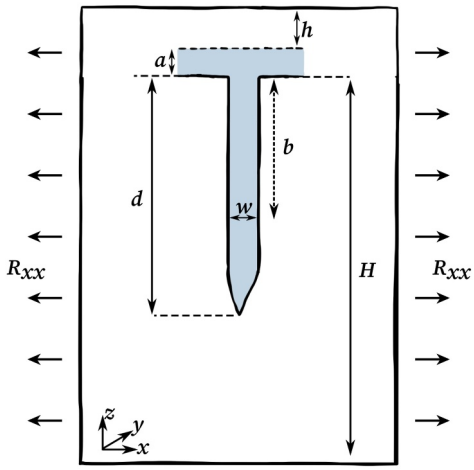

Figure 2. Schematic of fracture calculations. See text for symbol definitions. The line at the top of the fracture is the fracture surface. The dashed line indicates the top of the perched water body.

$$K^{(\mathrm{net})} = K^1 + K^2 + K^3. \quad (1)$$

The stress intensity factor corresponding to the tensile or compressive stress is given as

$$K^{(1)} = F(\lambda) R_{xx} \sqrt{\pi d} \quad (2)$$

where $\lambda = (d + h + a)/H, d$ (m) is the fracture depth, h is the height above the fracture surface (or water body surface if present) to the actual surface, a is the depth of the water body, and H is the ice shell thickness (Figure 2). This differs slightly from the setup in Van der Veen (2007) due to inclusion of a potentially deep perched water body and a potentially thick overlying ice lid and in this context, a and h are taken to be small relative to H. Rxx (Pa) is the resistive stress defined as

$$R_{xx} = \sigma_{xx} - L \quad (3)$$

where σ_{xx} (Pa) is the full stress and $L = -\rho_i g(H + h + a - z)$ (m) is the lithostatic stress where ρ_i (kg m^{-3}) is the density of ice, g (m s^{-2}) is acceleration due to gravity and z is 0 at the base of the ice shell increasing upwards. Values of R_{xx} will feature spatio-temporal variation but are likely at least locally extensive at the ice-shell surface (see Discussion for further details). $F(\lambda)$ is the shape factor accounting for the fracture geometry, calculated as

$$F(\lambda) = 1.12 - 0.23\lambda + 10.55\lambda^2 - 21.72\lambda^3 + 30.39\lambda^4 \quad (4)$$

following Van der Veen (1998) who draw from the compilation in Broek (1982, Table 3.1). This shape factor is intended for a fracture originating at the surface with a width to height ratio of 2 (Broek, 1988). Further consideration of a shape factor intended for a fracture originating in the middle of a plane, which reduces the value of $F(\lambda)$ for all positive values of λ, is Figure S1 in Supporting Information S1.

Next, the net stress intensity factor from the overburden pressure is calculated by integrating the contributions from forces acting at different depths as

$$K^{(2)} = -\frac{2g}{\sqrt{\pi d}} \int_0^d \left(\rho_i b + \rho_w a + \rho_i h\right) G(\gamma, \lambda) \mathrm{d}b \quad (5)$$

where the $\rho_w a$ and $\rho_i h$ account for the weight of overlying water and overlying mechanically strong lid respectively and ρ_w is the density of water, $\gamma = b/d$ and b is the depth from the fracture surface to the point in the fracture under consideration. I make the simplifying assumption that the ice lid is mechanically isolated from the water body and influences the hydrostatic stress (Equation 5) but not the water pressure (Equation 7). In reality, downwards freezing of the ice lid may pressurize the water body beyond the assumptions used here, though any pressure will be released following initial fracture creation and ice displacement. This simplification serves to illustrate the maximum fracture-limiting influence a lid overlying a perched water body may have. The shape function $G(\gamma, \lambda)$ is

$$G(\gamma,\lambda) = \frac{3.52(1-\gamma)}{(1-\lambda)^{3/2}} - \frac{4.35 - 5.28\gamma}{(1-\lambda)^{1/2}} + \left[\frac{1.30 - 0.30\gamma^{3/2}}{(1-\gamma^2)^{1/2}} + 0.83 - 1.76\gamma\right] \times [1 - (1-\gamma)\lambda] \quad (6)$$

which is obtained by Van der Veen (1998) from Tada et al. (2000, 2.29, p. 71) (Earlier editions of this textbook are difficult to locate so a more recent edition is cited. The equations are the same.).

Last, the stress intensity factor from the water pressure within the fracture following Van der Veen (1998) is

Table 1
Values Used in Calculations

Symbol	Value	Meaning
g	1.31 m s^{-2}	Gravitational acceleration
ν	0.3	Poisson's ratio
ρ_i	917 kg m^{-3}	Ice density
ρ_w	1,000 kg m^{-3}	Water density
μ	0.03, 0.3, 1.5 GPa	Shear modulus

Note. ν from Krawczynski et al. (2009), μ from Vaughan (1995).

$$K^{(3)} = \frac{2g}{\sqrt{\pi d}} \int_0^d \left(\rho_w b + \rho_w a\right) G(\gamma, \lambda) \mathrm{d}b. \tag{7}$$

$K^{(2)}$ and $K^{(3)}$ are then evaluated numerically to calculate $K^{(\mathrm{net})}$ at the given depth, d, using Equation 1.

Separately to Equations 1–7, the volume of water required for a given crack propagation depth is calculated following Krawczynski et al. (2009) and Weertman (1973). The fracture opening at a given depth is expressed as

$$w(b) = \frac{4\alpha\sigma}{\mu}\omega + \frac{4\alpha\rho_i g d}{\pi\mu}\omega - \frac{4\alpha\rho_w g}{\pi\mu}\omega\psi - \frac{2\alpha\rho_i g b^2}{\pi\mu} ln\left(\frac{d+\omega}{d-\omega}\right) + \frac{2\alpha\rho_w g\left(b^2 - a^2\right)}{\pi\mu} ln\left|\frac{\psi+\omega}{\psi-\omega}\right| - \frac{4\alpha\rho_w g b a}{\pi\mu} ln\left|\frac{a\omega + b\psi}{a\omega - b\psi}\right| + \frac{4\alpha\rho_w g a^2}{\pi\mu} ln\left|\frac{\omega+\psi}{\omega-\psi}\right| \tag{8}$$

where μ (Pa) is the shear modulus for ice, $\alpha = 1 - \nu$ where ν is Poisson's ratio, $\omega = \sqrt{d^2 - b^2}$ and $\psi = \sqrt{d^2 - a^2}$. In the application of Krawczynski et al. (2009) and Weertman (1973) the stress, σ, at depth d is calculated as

$$\sigma = R_{xx} - \frac{2\rho_i g d}{\pi} - \rho_w g a + \frac{\rho_w g a}{\pi} \sin^{-1}\left(\frac{a}{d}\right) + \frac{2\rho_w g}{\pi}\psi. \tag{9}$$

This approach is a simplification of the stress calculations in Equations 1–7 from Van der Veen (1998), but it is used here in keeping with Krawczynski et al. (2009) given its proven efficacy in the setting in which it is applied. The fracture volume required for full thickness hydrofracture is then

$$V_f = l \int_0^H w(b) \mathrm{d}b \tag{10}$$

which is evaluated numerically where l is the fracture length (along the y axis, into the page, and not displayed in Figure 2). Although the water body is approximated as plane in Equations 1–7 to calculate the water body volume I consider a spherical perched water body of radius r, the fracture length is then taken as $l = \frac{4}{3}r$. On Earth the fracture may at first span the diameter of the water body (Chudley et al., 2019), but a more spherical geometry would result in a shorter fracture length. The radius of the required sphere is

$$r = \sqrt{\frac{1}{\pi} \int_0^H w(b) \mathrm{d}b}. \tag{11}$$

Values used in calculations are provided in Table 1.

2. Results

The calculations demonstrate that under certain circumstances hydrofracture from a perched water body to the subsurface ocean of Europa is possible. Figure 3 shows the stress intensity experienced at the tip of the fracture against the fracture depth. If the stress intensity at the fracture tip exceeds the critical fracture toughness of ice the fracture will continue to propagate. If a mechanically strong lid is absent, that is, the lid is characterized as a weak layer of melange and slush, the rate of change of $K^{(3)}$ with depth exceeds that of $K^{(2)}$ for all depths considered (Figure S2 in Supporting Information S1) meaning that once the stress intensity factor at the fracture tip exceeds the critical fracture toughness the fracture will continue to propagate unbounded, limited only by the water supplying the fracture. An initial fracture depth of only 4.1 m under a tensile stress of 0.1 MPa is required for unstable hydrofracture if the water body is located on the surface. If an ice lid greater than around 100 m

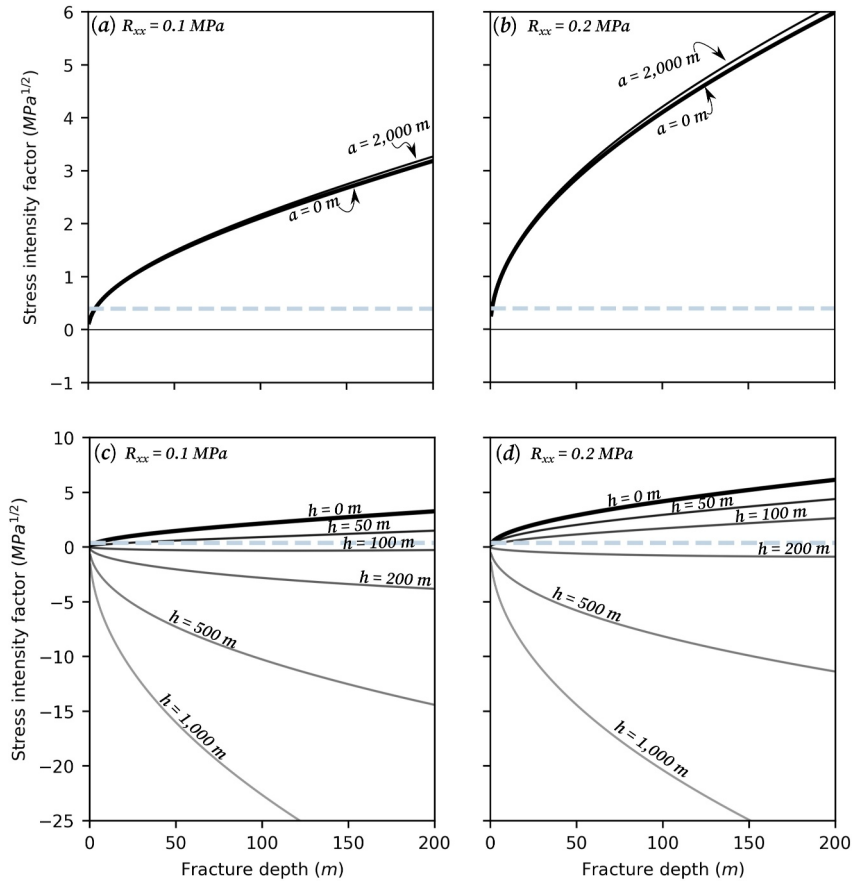

Figure 3. Stress intensity factor as function of fracture depth for varying ice lid thickness, water body depth, and tensile stress. The blue dashed line is a reasonable upper limit for the fracture toughness of ice (0.4 MPa $m^{1/2}$) from Van der Veen (1998). (a) and (b) The thickness of the overlying lid $h = 0$ m. (c) and (d) The depth of the water body $a = 500$ m. Panels (a) and (c) tensile stress is 0.1 MPa. (b) and (d) Tensile stress is 0.2 MPa. $H = 30$ km for all panels. Where the solid lines in panels (a)–(d) consistently increase above the fracture toughness unbounded hydrofracture can occur.

(dependent slightly on the value of a) is present that contributes to lithostatic but not hydrostatic pressure then the rate of change of $K^{(2)}$ with depth exceeds that of $K^{(3)}$ meaning fracture propagation is not favorable. Unreasonably deep initial fractures are required in the case of a surface water body and 0 MPa tensile stress but, once a fracture is established neutral far-field stress at depth would not lead to closure (Figure S3 in Supporting Information S1).

The volume of water required to facilitate a 30 km fracture under a shear modulus of 1.5 GPa is 38.8 km^3, or 570 km^3 for a shear modulus of 0.3 GPa (Figure 4). This is significantly below the 20,000–60,000 km^3 melt lens estimate of Schmidt et al. (2011) and around the same magnitude of melt volumes modeled to form by Kalousová et al. (2024) in the event of moderately sized meteorite impacts. Lower shear modulus values markedly increase the required water volume. Laboratory experiments suggest a shear modulus of ∼3.3 GPa for pure ice (Gammon et al., 1983), which may decrease to ∼0.3–1.7 GPa for metamorphosed meteoric ice (Godio & Rege, 2015; Vaughan, 1995). Nimmo and Schenk (2006) suggest 0.03–0.3 GPa for Europa based on analysis of normal faults, highlighting near-surface fracturing as a potential cause. A value at the upper end of Europa estimates may be more appropriate here however, as the fracture volume is mostly dependent on ice properties at depth within the shell. On Earth it is furthermore unclear the degree to which a fracture must maintain its width throughout propagation; by the time it is possible to conduct an investigation the passage is always narrow (Catania et al., 2008; Chudley et al., 2019).

Van der Veen (2007) shows that the key control on the downward propagation of the fracture is the filling rate and that penetration velocity equals the rate of fracture filling to within a few percent. This is because $K^{(2)}$ and $K^{(3)}$ become the dominant terms as depth increases giving to a good approximation

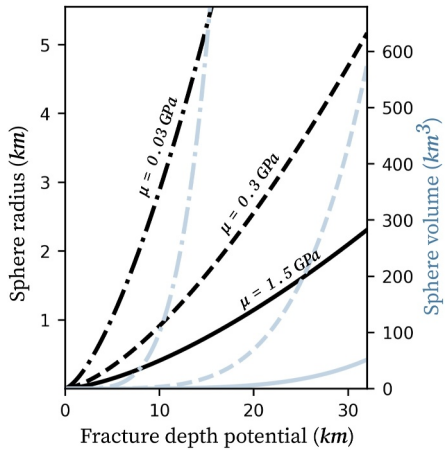

Figure 4. Water volume required for a given fracture depth. Dashed line is for a shear modulus of 0.5 GPa and solid line for 1.5 GPa. Note that the upper bound shear modulus of 3.9 GPa, as used in Krawczynski et al. (2009), is not included here. Black indicates required sphere radius, blue indicates sphere volume.

$$d = \left(\frac{\rho_w}{\rho_i}\right)^{\frac{2}{5}} Qt \tag{12}$$

where Q is the vertical fill rate (m s^{-1}) and t (s) is the time period in consideration. Hydrofracture could therefore be a very rapid phenomenon given a suitably placed large perched water body. Supraglacial lakes in Greenland take on the order of 2–3 hr to drain, but the water bodies have an aspect ratio of 1:100 making Q limited by lateral transport from the outer reaches of the lake (Chudley et al., 2019; Das et al., 2008). As a first approximation, even if drainage took 24 hr through ice at 100 K, only 0.34 m of side wall freezing would occur (Text S2 in Supporting Information S1), negligible in the context of a surface opening of ∼200 m following Equation 8.

3. Discussion

Figures 3 and 4 demonstrate that full hydrofracture of Europa is possible given moderate tensile stresses, sufficient water to propagate the fracture, and a lid comprised of an ice melange lacking functional mechanical strength. Fractures are common across Europa's surface (e.g., Dombard et al., 2013) but abundant surface water akin to the Greenland Ice Sheet is practically impossible given the very low temperature and pressure of the ice surface (Ashkenazy, 2019). Nonetheless, in this simple if unrealistic situation, hydrofracture can occur at tensile stresses much lower than the >20 MPa proposed by Crawford and Stevenson (1988) and Rudolph and Manga (2009) for full "dry" shell fracture. As for any planetary body, it is challenging to quantify the surface and depth-averaged stress state of Europa. However, estimates for the surface are around the 0.1–0.2 MPa, with regions of compression and extension both expected (Greenberg et al., 2002; Hoppa et al., 1999; Kattenhorn & Marshall, 2006; Pappalardo et al., 1998). Cooling and freezing of liquid water to the ice shell base may furthermore lead to extensive extension throughout the ice shell (Nimmo, 2004). As with Antarctic ice shelves and the Greenland Ice Sheet, hydrofracture of perched water bodies may therefore only occur under spatially or temporally limited stress conditions.

However if, as widely hypothesized (Fagents et al., 2022), a water body is entombed then the additional lithostatic stress and fracture stress configuration makes rapid hydrofracture (or any Mode I fracture at all) unlikely. Though it is worth noting that mechanisms hypothesized to direct water upwards such as the pressurization through freezing of perched water bodies (Lesage et al., 2022; Manga & Wang, 2007; Quick et al., 2023; Steinbrügge et al., 2020), ought also to work downwards and will be aided in that case by density-difference driven fracture. But, if the lid is comprised of weak melange then its weight will contribute to the hydrostatic pressure and not the lithostatic pressure and hydrofracture again becomes possible. Two such scenarios may occur.

First, Schmidt et al. (2011), Walker and Schmidt (2015), and Luzzi et al. (2021) among others propose collapse of the upper shell above perched water bodies as a formation mechanism for chaos terrains. In several of these scenarios, the blocks of ice are buoyantly supported by brine, water, and slush (Figure 1c). This effectively sets h at zero, while increasing a, meaning hydrofracture becomes a realistic possibility. It is unclear how long this lid state may persist before refreezing occurs (Fagents et al., 2022; Schmidt et al., 2011), but while it does only a small and temporary tensile stress and a very small initial fracture would be required to initiate rapid hydrofracture.

Second, literature on the impacts of meteor impacts on icy moons is limited, but it appears reasonable that an impactor may provide three ingredients for hydrofracture—an initial fracture site, a tensile shock, and an abundant supply of impact-generated melt water (Kalousová et al., 2024) while leaving an at least transiently mechanically weak area above the water body (Figure 1f). A meteorite may also impact sufficiently close to an existing perched water body to trigger its hydrofracture, though meteorite impacts have also been invoked as a potential cause of cryovolcanism (Steinbrügge et al., 2020). If density driven sinking of melt (Carnahan et al., 2022; Kalousová et al., 2024) actually prevents the formation of a perched water body, then a meteorite impact becomes the only remaining possible source of a large water body.

If a previously entombed water body drains, the drainage event will remove hydrostatic support and lead to extensive collapse of the overlying terrain. If the fracture remains open the water level would then be expected to stabilize at ∼90% of the ice shell thickness (Michaut & Manga, 2014), though viscous deformation and freezing may be expected to close the fracture over a short period (years or less) after active drainage has ceased (Andrews et al., 2022). It is worth noting that in Greenland the large ice blocks generated in initial hydrofracture, with more expected if an icy lid is present (Russell, 1993), may become wedged at the fracture surface (Figure S4 in Supporting Information S1) so while water may leave the site quickly, solid ice blocks should remain. This supports a more neocatastrophist view of chaos terrain formation than gradual collapse of the upper shell (Luzzi et al., 2021).

Last, it is challenging to be definitive about the thermal state of Europa's icy shell, but several studies suggest a warm and uniform convecting interior, within around 10 K of the pressure melting point (e.g., Hussmann et al., 2002; McKinnon, 1999; Mitri & Showman, 2005; Showman & Han, 2004). These temperatures are warm relative to an average surface temperature of around 100 K (Ashkenazy, 2019), but their correspondingly lower relative viscosity should not present a problem to elastic fracture given full-thickness hydrofracture through ice of this temperature is common in the Greenland Ice Sheet (e.g., Doyle et al., 2018; Law et al., 2021). More intriguing is the possible influence of temperate ice on water transport within Europa's shell. Carnahan et al. (2022) and Kalousová et al. (2024) do not account for the formation of conduits within the icy shell, yet there are no temperate terrestrial glaciers where there is not some degree of englacial drainage system formation (e.g., Hooke, 1989). A body of temperate ice within an icy shell would lack a supply of surface meltwater, but tidal or convective heating may still produce water internally (e.g., Gaidos & Nimmo, 2000). Given that the melt chambers hypothesized by Carnahan et al. (2022) reach >5 km in height and feature melt fractions >5%, it seems reasonable that transport through a drainage system may lead to pooling of water at the transition between temperate and cold ice if fracture does not occur. Further integrating understanding of englacial hydrology with icy moon mechanics can advance understanding of these mechanisms.

4. Conclusions

This paper demonstrates that in the presence of a mechanically weak lid only relatively small tensile stresses, and achievable water volumes, are required for full hydrofracture of Europa's ice shell. This has direct application to other icy moons with different gravities and stress regimes, which may also have conditions facilitating full-thickness hydrofracture. It also provides a clear mechanism for the delivery to the subsurface ocean of biologically important materials created on the surface of Europa and delivered by incoming meteorites and may provide an explanation for the formation of chaos terrains. Future research directions include numerical modeling of the spatio-temporal variation of stress configurations around varied perched water body geometries (Craft et al., 2023; Hageman et al., 2024) and as a result of meteorite impacts, and improving understanding of the geomorphological implications of rapid hydrofracture. Hopefully, this paper opens further interdisciplinary pathways (Garcia-Lopez & Cid, 2017; Rossi et al., 2023) between glaciology and the study of icy moons.

Conflict of Interest

The authors declare no conflicts of interest relevant to this study.

Data Availability Statement

The data supporting the conclusions is derived from the calculations outlined in the text. Plotting and analysis scripts, which produce the derived data, are available at Law (2024).

Acknowledgments
Thanks to Craig Walton and Claire Guimond for introducing me to this field and Andreas Born for letting me take a bit of time away from the day job. Thanks to two anonymous reviewers for very helpful comments. I acknowledge funding from The Research Council of Norway (Norges Forskningsråd) Grant 314614 (Simulating Ice Cores and Englacial Tracers in the Greenland Ice Sheet).

References

Andrews, L. C., Poinar, K., & Trunz, C. (2022). Controls on Greenland moulin geometry and evolution from the Moulin Shape model. *The Cryosphere*, *16*(6), 2421–2448. https://doi.org/10.5194/TC-16-2421-2022

Ashkenazy, Y. (2019). The surface temperature of Europa. *Heliyon*, *5*(6), 1908. https://doi.org/10.1016/j.heliyon.2019.e01908

Banwell, A. F., MacAyeal, D. R., & Sergienko, O. V. (2013). Breakup of the Larsen B Ice Shelf triggered by chain reaction drainage of supraglacial lakes. *Geophysical Research Letters*, *40*(22), 5872–5876. https://doi.org/10.1002/2013GL057694

Banwell, A. F., Willis, I. C., Stevens, L. A., Dell, R. L., & Macayeal, D. R. (2024). Observed meltwater-induced flexure and fracture at a doline on George VI Ice Shelf, Antarctica. *Journal of Glaciology*, *70*, e47. https://doi.org/10.1017/JOG.2024.31

Billings, S. E., & Kattenhorn, S. A. (2005). The great thickness debate: Ice shell thickness models for Europa and comparisons with estimates based on flexure at ridges. *Icarus*, *177*(2), 397–412. https://doi.org/10.1016/J.ICARUS.2005.03.013

Broek, D. (1982). Elementary engineering fracture mechanics. *Elementary engineering fracture mechanics*. https://doi.org/10.1007/978-94-009-4333-9

Broek, D. (1988). *The practical use of fracture mechanics* (1st ed.). Springer. https://doi.org/10.1007/978-94-009-2558-8

Carlson, R. W., Anderson, M. S., Johnson, R. E., Smythe, W. D., Hendrix, A. R., Barth, C. A., et al. (1999). Hydrogen peroxide on the surface of Europa. *Science*, *283*(5410), 2062–2064. https://doi.org/10.1126/SCIENCE.283.5410.2062

Carnahan, E., Vance, S. D., Cox, R., & Hesse, M. A. (2022). Surface-to-ocean exchange by the sinking of impact generated melt chambers on Europa. *Geophysical Research Letters*, *49*(24), e2022GL100287. https://doi.org/10.1029/2022GL100287

Carr, M. H., Belton, M. J., Chapman, C. R., Davies, M. E., Geissler, P., Greenberg, R., et al. (1998). Evidence for a subsurface ocean on Europa. *Nature*, *391*(6665), 363–365. https://doi.org/10.1038/34857

Catania, G. A., Neumann, T. A., & Price, S. F. (2008). Characterizing englacial drainage in the ablation zone of the Greenland ice sheet. *Journal of Glaciology*, *54*(187), 567–578. https://doi.org/10.3189/002214308786570854

Christoffersen, P., Bougamont, M., Hubbard, A., Doyle, S. H., Grigsby, S., & Pettersson, R. (2018). Cascading lake drainage on the Greenland Ice Sheet triggered by tensile shock and fracture. *Nature Communications*, *9*(1), 1064. https://doi.org/10.1038/s41467-018-03420-8

Chudley, T. R., Christoffersen, P., Doyle, S., Bougamont, M., Schoonman, C., Hubbard, B., & James, M. (2019). Supraglacial lake drainage at a fast-flowing Greenlandic outlet glacier. *Proceedings of the National Academy of Sciences of the United States of America*, *116*(51), 25468–25477. https://doi.org/10.1073/pnas.1913685116

Chudley, T. R., Christoffersen, P., Doyle, S. H., Dowling, T. P., Law, R., Schoonman, C. M., et al. (2021). Controls on water storage and drainage in crevasses on the Greenland ice sheet. *Journal of Geophysical Research: Earth Surface*, *126*(9), e2021JF006287. https://doi.org/10.1029/2021JF006287

Chyba, C. F. (2000). Energy for microbial life on Europa. *Nature*, *403*(6768), 381–382. https://doi.org/10.1038/35000281

Chyba, C. F., & Phillips, C. B. (2001). Possible ecosystems and the search for life on Europa. *Proceedings of the National Academy of Sciences of the United States of America*, *98*(3), 801–804. https://doi.org/10.1073/pnas.98.3.801

Collins, G. C., Head, J. W., Pappalardo, R. T., & Spaun, N. A. (2000). Evaluation of models for the formation of chaotic terrain on Europa. *Journal of Geophysical Research*, *105*(E1), 1709–1716. https://doi.org/10.1029/1999JE001143

Cooley, S. W., & Christoffersen, P. (2017). Observation bias correction reveals more rapidly draining lakes on the Greenland Ice Sheet. *Journal of Geophysical Research: Earth Surface*, *122*(10), 1867–1881. https://doi.org/10.1002/2017JF004255

Craft, K. L., Chen, A. E., Rhoden, A. R., & MacKenzie, S. M. (2023). Impact induced fracture propagation through ice on ocean worlds. In *Workshop on ICES in the Solar System*.

Craft, K. L., Patterson, G. W., Lowell, R. P., & Germanovich, L. (2016). Fracturing and flow: Investigations on the formation of shallow water sills on Europa. *Icarus*, *274*, 297–313. https://doi.org/10.1016/j.icarus.2016.01.023

Crawford, G. D., & Stevenson, D. J. (1988). Gas-driven water volcanism and the resurfacing of Europa. *Icarus*, *73*(1), 66–79. https://doi.org/10.1016/0019-1035(88)90085-1

Das, S. B., Joughin, I., Behn, M. D., Howat, I. M., King, M. A., Lizarralde, D., & Bhatia, M. P. (2008). Fracture propagation to the base of the Greenland Ice Sheet during supraglacial lake drainage. *Science*, *320*(5877), 778–781. https://doi.org/10.1126/science.1153360

Delitsky, M. L., & Lane, A. L. (1998). Ice chemistry on the Galilean satellites. *Journal of Geophysical Research*, *103*(E13), 31391–31403. https://doi.org/10.1029/1998JE900020

Dombard, A. J., Patterson, G. W., Lederer, A. P., & Prockter, L. M. (2013). Flanking fractures and the formation of double ridges on Europa. *Icarus*, *223*(1), 74–81. https://doi.org/10.1016/J.ICARUS.2012.11.021

Doyle, S. H., Hubbard, A. L., Dow, C. F., Jones, G. A., Fitzpatrick, A., Gusmeroli, A., et al. (2013). Ice tectonic deformation during the rapid in situ drainage of a supraglacial lake on the Greenland Ice Sheet. *The Cryosphere*, *7*(1), 129–140. https://doi.org/10.5194/tc-7-129-2013

Doyle, S. H., Hubbard, B., Christoffersen, P., Young, T. J., Hofstede, C., Bougamont, M., et al. (2018). Physical conditions of fast glacier flow: 1. Measurements from boreholes drilled to the bed of store glacier, West Greenland. *Journal of Geophysical Research: Earth Surface*, *123*(2), 324–348. https://doi.org/10.1002/2017JF004529

Dunmire, D., Lenaerts, J. T., Banwell, A. F., Wever, N., Shragge, J., Lhermitte, S., et al. (2020). Observations of buried lake drainage on the Antarctic Ice Sheet. *Geophysical Research Letters*, *47*(15), e2020GL087970. https://doi.org/10.1029/2020GL087970

Fagents, S. A., Lopes, R. M., Quick, L. C., & Gregg, T. K. (2022). Cryovolcanism, *Planetary Volcanism across the Solar System* (pp. 161–234). https://doi.org/10.1016/B978-0-12-813987-5.00005-5

Figueredo, P. H., Chuang, F. C., Rathbun, J., Kirk, R. L., & Greeley, R. (2002). Geology and origin of Europa's "Mitten" feature (Murias Chaos). *Journal of Geophysical Research*, *107*(E5). https://doi.org/10.1029/2001JE001591

Fitzpatrick, A. A. W., Hubbard, A. L., Box, J. E., Quincey, D. J., van As, D., Mikkelsen, A. P. B., et al. (2014). A decade (2002-2012) of supraglacial lake volume estimates across Russell Glacier, West Greenland. *The Cryosphere*, *8*(1), 107–121. https://doi.org/10.5194/tc-8-107-2014

Fountain, A. G., & Walder, J. S. (1998). Water flow through temperate glaciers. *Reviews of Geophysics*, *36*(3), 299–328. https://doi.org/10.1029/97RG03579

Gaidos, E. J., & Nimmo, F. (2000). Tectonics and water on Europa. *Nature*, *405*(6787), 637–637. https://doi.org/10.1038/35015170

Gammon, P. H., Kiefte, H., Clouter, M. J., & Denner, W. W. (1983). Elastic constants of artificial and natural ice samples by Brillouin spectroscopy. *Journal of Glaciology*, *29*(103), 433–460. https://doi.org/10.3189/S0022143000030355

Garcia-Lopez, E., & Cid, C. (2017). Glaciers and ice sheets as analog environments of potentially habitable icy worlds. *Frontiers in Microbiology*, *8*, 267284. https://doi.org/10.3389/FMICB.2017.01407/BIBTEX

Godio, A., & Rege, R. B. (2015). The mechanical properties of snow and ice of an alpine glacier inferred by integrating seismic and GPR methods. *Journal of Applied Geophysics*, *115*, 92–99. https://doi.org/10.1016/J.JAPPGEO.2015.02.017

Goldsby, D. L., & Kohlstedt, D. L. (2001). Superplastic deformation of ice: Experimental observations. *Journal of Geophysical Research*, *106*(B6), 11017–11030. https://doi.org/10.1029/2000jb900336

Goodman, J. C., Collins, G. C., Marshall, J., & Pierrehumbert, R. T. (2004). Hydrothermal plume dynamics on Europa: Implications for chaos formation. *Journal of Geophysical Research*, *109*(E3), E03008. https://doi.org/10.1029/2003JE002073

Greenberg, R., Geissler, P., Hoppa, G., & Tufts, B. R. (2002). Tidal-tectonic processes and their implications for the character of Europa's icy crust. *Reviews of Geophysics*, *40*(2), 1-1–1-33. https://doi.org/10.1029/2000RG000096

Griffits, A. A. (1921). VI. The phenomena of rupture and flow in solids. *Philosophical Transactions of the Royal Society of London. Series A, Containing Papers of a Mathematical or Physical Character*, *4*(1), 9–14. https://doi.org/10.1098/RSTA.1921.0006

Gulley, J. D., Benn, D. I., Mu¨ller, D., Mu¨ller, M., & Luckman, A. (2009). A cut-and-closure origin for englacial conduits in uncrevassed regions of polythermal glaciers. *Journal of Glaciology*, *55*(189), 66–80. https://doi.org/10.3189/002214309788608930

Hageman, T., Mejía, J., Duddu, R., & Martínez-Pañeda, E. (2024). Ice viscosity governs hydraulic fracture that causes rapid drainage of supraglacial lakes. *The Cryosphere*, *18*(9), 3991–4009. https://doi.org/10.5194/TC-18-3991-2024

Hendrix, A. R., Hurford, T. A., Barge, L. M., Bland, M. T., Bowman, J. S., Brinckerhoff, W., et al. (2019). The NASA Roadmap to ocean worlds. *Astrobiology*, *19*(1), 1–27. https://doi.org/10.1089/ast.2018.1955

Hesse, M. A., Jordan, J. S., Vance, S. D., & Oza, A. V. (2022). Downward oxidant transport through Europa's Ice Shell by Density-driven brine percolation. *Geophysical Research Letters*, *49*(5), e2021GL095416. https://doi.org/10.1029/2021GL095416

Hooke, R. (1989). Englacial and subglacial hydrology: A qualitative review. *Arctic and Alpine Research*, *21*(3), 221–233. https://doi.org/10.1080/00040851.1989.12002734

Hoppa, G. V., Tufts, B. R., Greenberg, R., & Geissler, P. E. (1999). Formation of cycloidal features on Europa. *Science*, *285*(5435), 1899–1902. https://doi.org/10.1126/science.285.5435.1899

Hussmann, H., Spohn, T., & Wieczerkowski, K. (2002). Thermal equilibrium states of Europa's ice shell: Implications for internal ocean thickness and surface heat flow. *Icarus*, *156*(1), 143–151. https://doi.org/10.1006/ICAR.2001.6776

Kalousová, K., Wakita, S., Sotin, C., Neish, C. D., Soderblom, J. M., Souček, O., & Johnson, B. C. (2024). Evolution of impact melt pools on Titan. *Journal of Geophysical Research: Planets*, *129*(3), e2023JE008107. https://doi.org/10.1029/2023JE008107

Kargel, J. S., Kaye, J. Z., Head, J. W., Marion, G. M., Sassen, R., Crowley, J. K., et al. (2000). Europa's crust and ocean: Origin, composition, and the prospects for life. *Icarus*, *148*(1), 226–265. https://doi.org/10.1006/ICAR.2000.6471

Karlstrom, L., Zok, A., & Manga, M. (2014). Near-surface permeability in a supraglacial drainage basin on the Llewellyn Glacier, Juneau Icefield, British Columbia. *The Cryosphere*, *8*(2), 537–546. https://doi.org/10.5194/tc-8-537-2014

Kattenhorn, S. A., & Marshall, S. T. (2006). Fault-induced perturbed stress fields and associated tensile and compressive deformation at fault tips in the ice shell of Europa: Implications for fault mechanics. *Journal of Structural Geology*, *28*(12), 2204–2221. https://doi.org/10.1016/J.JSG.2005.11.010

Khurana, K. K., Kivelson, M. G., Stevenson, D. J., Schubert, G., Russell, C. T., Walker, R. J., & Polanskey, C. (1998). Induced magnetic fields as evidence for subsurface oceans in Europa and Callisto. *Nature*, *395*(6704), 777–780. https://doi.org/10.1038/27394

Krawczynski, M. J., Behn, M. D., Das, S. B., & Joughin, I. (2009). Constraints on the lake volume required for hydro-fracture through ice sheets. *Geophysical Research Letters*, *36*(10), L10501. https://doi.org/10.1029/2008GL036765

Law, R. (2024). Replication data for: Rapid hydrofracture of icy moon shells: Insights from glaciology v1. *Harvard Dataverse*. https://doi.org/10.7910/DVN/ODVYL2

Law, R., Christoffersen, P., Hubbard, B., Doyle, S. H., Chudley, T. R., Schoonman, C., et al. (2021). Thermodynamics of a fast-moving Greenlandic outlet glacier revealed by fiber-optic distributed temperature sensing. *Science Advances*, *7*(20), eabe7136. https://doi.org/10.1126/sciadv.abe7136

Lee, S., Pappalardo, R. T., & Makris, N. C. (2005). Mechanics of tidally driven fractures in Europa's ice shell. *Icarus*, *177*(2), 367–379. https://doi.org/10.1016/j.icarus.2005.07.003

Lesage, E., Massol, H., Howell, S. M., & Schmidt, F. (2022). Simulation of freezing Cryomagma Reservoirs in viscoelastic ice shells. *The Planetary Science Journal*, *3*(7), 170. https://doi.org/10.3847/PSJ/AC75BF

Lewis, J. S. (1971). Satellites of the outer planets: Their physical and chemical nature. *Icarus*, *15*(2), 174–185. https://doi.org/10.1016/0019-1035(71)90072-8

Lorenz, R. D., Stiles, B. W., Kirk, R. L., Allison, M. D., Del Marmo, P. P., Iess, L., et al. (2008). Titan's rotation reveals an internal ocean and changing zonal winds. *Science*, *319*(5870), 1649–1651. https://doi.org/10.1126/science.1151639

Luzzi, E., Rossi, A. P., Massironi, M., Pozzobon, R., Corti, G., & Maestrelli, D. (2021). Caldera collapse as the trigger of chaos and fractured Craters on the Moon and Mars. *Geophysical Research Letters*, *48*(11), e2021GL092436. https://doi.org/10.1029/2021GL092436

Manga, M., & Wang, C. Y. (2007). Pressurized oceans and the eruption of liquid water on Europa and Enceladus. *Geophysical Research Letters*, *34*(7), L07202. https://doi.org/10.1029/2007GL029297

McKinnon, W. B. (1999). Convective instability in Europa's floating ice shell. *Geophysical Research Letters*, *26*(7), 951–954. https://doi.org/10.1029/1999GL900125

Michaut, C., & Manga, M. (2014). Domes, pits, and small chaos on Europa produced by water sills. *Journal of Geophysical Research: Planets*, *119*(3), 550–573. https://doi.org/10.1002/2013JE004558

Mitri, G., & Showman, A. P. (2005). Convective–conductive transitions and sensitivity of a convecting ice shell to perturbations in heat flux and tidal-heating rate: Implications for Europa. *Icarus*, *177*(2), 447–460. https://doi.org/10.1016/J.ICARUS.2005.03.019

NASA. (2017). *Europa Lander Study 2016 Report* (Technical Report). NASA. Retrieved from https://europa.nasa.gov/resources/58/europa-lander-study-2016-report/

Nimmo, F. (2004). Stresses generated in cooling viscoelastic ice shells: Application to Europa. *Journal of Geophysical Research*, *109*(E12), E12001. https://doi.org/10.1029/2004JE002347

Nimmo, F., & Schenk, P. (2006). Normal faulting on Europa: Implications for ice shell properties. *Journal of Structural Geology*, *28*(12), 2194–2203. https://doi.org/10.1016/J.JSG.2005.08.009

Pappalardo, R. T., & Barr, A. C. (2004). The origin of domes on Europa: The role of thermally induced compositional diapirism. *Geophysical Research Letters*, *31*(1), L01701. https://doi.org/10.1029/2003GL019202

Pappalardo, R. T., Head, J. W., Greeley, R., Sullivan, R. J., Pilcher, C., Schubert, G., et al. (1998). Geological evidence for solid-state convection in Europa's ice shell. *Nature*, *391*(6665), 365–368. https://doi.org/10.1038/34862

Poinar, K., & Andrews, L. (2021). Challenges in predicting Greenland supraglacial lake drainages at the regional scale. *The Cryosphere*, *15*(3), 1455–1483. https://doi.org/10.5194/TC-15-1455-2021

Poinelli, M., Larour, E., Castillo-Rogez, J., & Vermeersen, B. (2019). Crevasse propagation on brittle ice: Application to Cycloids on Europa. *Geophysical Research Letters*, *46*(21), 11756–11763. https://doi.org/10.1029/2019GL084033

Porco, C. C., Helfenstein, P., Thomas, P. C., Ingersoll, A. P., Wisdom, J., West, R., et al. (2006). Cassini observes the active south pole of enceladus. *Science*, *311*(5766), 1393–1401. https://doi.org/10.1126/science.1123013

Quick, L. C., Roberge, A., Mendoza, G. T., Quintana, E. V., & Youngblood, A. A. (2023). Prospects for cryovolcanic activity on cold ocean planets. *The Astrophysical Journal*, *956*(1), 29. https://doi.org/10.3847/1538-4357/ace9b6

Robel, A. A., & Banwell, A. F. (2019). A speed limit on ice shelf collapse through hydrofracture. *Geophysical Research Letters*, *46*(21), 12092–12100. https://doi.org/10.1029/2019GL084397

Rossi, C., Cianfarra, P., Lucchetti, A., Pozzobon, R., Penasa, L., Munaretto, G., & Pajola, M. (2023). Deformation patterns of icy satellite crusts: Insights for tectonic balancing and fluid migration through structural analysis of terrestrial analogues. *Icarus*, *404*, 115668. https://doi.org/10.1016/J.ICARUS.2023.115668

Rudolph, M. L., & Manga, M. (2009). Fracture penetration in planetary ice shells. *Icarus*, *199*(2), 536–541. https://doi.org/10.1016/J.ICARUS.2008.10.010

Russell, A. J. (1993). Supraglacial lake drainage near Sendre Strømjjord, Greenland. *Journal of Glaciology*, *39*(132), 431–433. https://doi.org/10.3189/s0022143000016105

Scambos, T. A., Hulbe, C., Fahnestock, M., & Bohlander, J. (2000). The link between climate warming and break-up of ice shelves in the Antarctic Peninsula. *Journal of Glaciology*, *46*(154), 516–530. https://doi.org/10.3189/172756500781833043

Schenk, P. M. (2002). Thickness constraints on the icy shells of the galilean satellites from a comparison of crater shapes. *Nature*, *417*(6887), 419–421. https://doi.org/10.1038/417419a

Schmidt, B. E., Blankenship, D. D., Patterson, G. W., & Schenk, P. M. (2011). Active formation of 'chaos terrain' over shallow subsurface water on Europa. *Nature*, *479*(7374), 502–505. https://doi.org/10.1038/nature10608

Sephton, M. A., Waite, J. H., & Brockwell, T. G. (2018). How to detect life on icy moons. *Astrobiology*, *18*(7), 843–855. https://doi.org/10.1089/ast.2017.1656

Showman, A. P., & Han, L. (2004). Numerical simulations of convection in Europa's ice shell: Implications for surface features. *Journal of Geophysical Research*, *109*(E1), E01010. https://doi.org/10.1029/2003je002103

Singer, K. N., McKinnon, W. B., & Schenk, P. M. (2023). Thin ice lithospheres and high heat flows on Europa from large impact structure Ring-Graben. *Journal of Geophysical Research: Planets*, *128*(12), e2023JE007928. https://doi.org/10.1029/2023JE007928

Sotin, C., Head, J. W., & Tobie, G. (2002). Europa: Tidal heating of upwelling thermal plumes and the origin of lenticulae and chaos melting. *Geophysical Research Letters*, *29*(8), 74-1–74-4. https://doi.org/10.1029/2001GL013844

Steinbrügge, G., Voigt, J. R., Wolfenbarger, N. S., Hamilton, C. W., Soderlund, K. M., Young, D. A., et al. (2020). Brine migration and impact-induced cryovolcanism on Europa. *Geophysical Research Letters*, *47*(21), e2020GL090797. https://doi.org/10.1029/2020GL090797

Stevens, L. A., Behn, M. D., McGuire, J. J., Das, S. B., Joughin, I., Herring, T., et al. (2015). Greenland supraglacial lake drainages triggered by hydrologically induced basal slip. *Nature*, *522*(7554), 73–76. https://doi.org/10.1038/nature14480

Tada, H., Paris, P. C., & Irwin, G. R. (2000). *The Stress Analysis of Cracks Handbook* (3rd ed.). ASME Press. https://doi.org/10.1115/1.801535

Thomson, R. E., & Delaney, J. R. (2001). Evidence for a weakly stratified Europan ocean sustained by seafloor heat flux. *Journal of Geophysical Research*, *106*(6), 12355–12365. https://doi.org/10.1029/2000je001332

Todd, J., & Christoffersen, P. (2014). Are seasonal calving dynamics forced by buttressing from ice mélange or undercutting by melting? Outcomes from full-Stokes simulations of Store Glacier, West Greenland. *The Cryosphere*, *8*(6), 2353–2365. https://doi.org/10.5194/TC-8-2353-2014

Van der Veen, C. J. (1998). Fracture mechanics approach to penetration of surface crevasses on glaciers. *Cold Regions Science and Technology*, *27*(1), 31–47. https://doi.org/10.1016/S0165-232X(97)00022-0

Van der Veen, C. J. (2007). Fracture propagation as means of rapidly transferring surface meltwater to the base of glaciers. *Geophysical Research Letters*, *34*(1), L01501. https://doi.org/10.1029/2006GL028385

Van der Veen, C. J. (2013). *Fundamentals of glacier dynamics* (2nd ed.). CRC Press. https://www.taylorfrancis.com/books/mono/10.1201/b14059/fundamentals-glacier-dynamics-van-der-veen

Vaughan, D. G. (1995). Tidal flexure at ice shelf margins. *Journal of Geophysical Research*, *100*(B4), 6213–6224. https://doi.org/10.1029/94JB02467

Walker, C. C., Bassis, J. N., & Schmidt, B. E. (2021). Propagation of vertical fractures through planetary ice shells: The role of basal fractures at the ice–ocean interface and proximal cracks. *The Planetary Science Journal*, *2*(4), 135. https://doi.org/10.3847/PSJ/AC01EE

Walker, C. C., & Schmidt, B. E. (2015). Ice collapse over trapped water bodies on Enceladus and Europa. *Geophysical Research Letters*, *42*(3), 712–719. https://doi.org/10.1002/2014GL062405

Warner, R. C., Fricker, H. A., Adusumilli, S., Arndt, P., Kingslake, J., & Spergel, J. J. (2021). Rapid formation of an ice doline on Amery Ice Shelf, East Antarctica. *Geophysical Research Letters*, *48*(14), e2020GL091095. https://doi.org/10.1029/2020GL091095

Weertman, J. (1973). Can a water-filled crevasse reach the bottom surface of a glacier. *International Association of Scientific Hydrology*, *95*, 139–145.

Williamson, A. G., Banwell, A. F., Willis, I. C., & Arnold, N. S. (2018). Dual-satellite (Sentinel-2 and Landsat 8) remote sensing of supraglacial lakes in Greenland. *The Cryosphere Discussions*, 1–27. https://doi.org/10.5194/tc-2018-56

Williamson, A. G., Willis, I. C., Arnold, N. S., & Banwell, A. F. (2018). Controls on rapid supraglacial lake drainage in West Greenland: An Exploratory data analysis approach. *Journal of Glaciology*, *64*(244), 208–226. https://doi.org/10.1017/jog.2018.8

References From the Supporting Information

Alley, R. B., Dupont, T. K., Parizek, B. R., & Anandakrishnan, S. (2005). Access of surface meltwater to beds of sub-freezing glaciers: Preliminary insights. *Annals of Glaciology*, *40*, 8–14. https://doi.org/10.3189/172756405781813483

Cuffey, K. M., & Paterson, W. S. B. (2010). *The physics of glaciers* (4th ed.). Elsevier Science & Technology Books.

Rubin, A. M. (1995). Propagation of magma-filled cracks. *Annual Review of Earth and Planetary Sciences*, *23*(1), 287–336. https://doi.org/10.1146/annurev.earth.23.1.287